One-step DNA melting in the RNA polymerase cleft opens the initiation bubble to form an unstable open complex

Theodore J. Gries[a], Wayne S. Kontur[b,2], Michael W. Capp[a], Ruth M. Saecker[a,1], and M. Thomas Record, Jr.[a,b,1]

[a]Department of Biochemistry, University of Wisconsin, 433 Babcock Drive, Madison, WI 53706; and [b]Department of Chemistry, University of Wisconsin, 1101 University Avenue, Madison, WI 53706

Edited* by E. Peter Geiduschek, University of California at San Diego, La Jolla, CA, and approved April 13, 2010 (received for review January 24, 2010)

Though opening of the start site (+1) region of promoter DNA is required for transcription by RNA polymerase (RNAP), surprisingly little is known about how and when this occurs in the mechanism. Early events at the λP_R promoter load this region of duplex DNA into the active site cleft of *Escherichia coli* RNAP, forming the closed, permanganate-unreactive intermediate I_1. Conversion to the subsequent intermediate I_2 overcomes a large enthalpic barrier. Is I_2 open? Here we create a burst of I_2 by rapidly destabilizing open complexes (RP_o) with 1.1 M NaCl. Fast footprinting reveals that thymines at positions from −11 to +2 in I_2 are permanganate-reactive, demonstrating that RNAP opens the entire initiation bubble in the cleft in a single step. Rates of decay of all observed thymine reactivities are the same as the I_2 to I_1 conversion rate determined by filter binding. In I_2, permanganate reactivity of the +1 thymine on the template (t) strand is the same as the RP_o control, whereas nontemplate (nt) thymines are significantly less reactive than in RP_o. We propose that: (*i*) the +1(t) thymine is in the active site in I_2; (*ii*) conversion of I_2 to RP_o repositions the nt strand in the cleft; and (*iii*) movements of the nt strand are coupled to the assembly and DNA binding of the downstream clamp and jaw that occurs after DNA opening and stabilizes RP_o. We hypothesize that unstable open intermediates at the λP_R promoter resemble the unstable, transcriptionally competent open complexes formed at ribosomal promoters.

bottleneck step | transcription regulation | burst experiment | protein nucleic acid interactions

Interactions between RNA polymerase and specific promoter DNA sequences trigger a precise progression of conformational changes in both biomolecules. Taken together, these steps constitute the mechanism of DNA opening and the start of the transcription cycle. For *Escherichia coli* RNA polymerase holoenzyme (RNAP, subunit composition: $\alpha_2\beta\beta'\omega\sigma^{70}$), binding free energy drives opening of the initiation bubble (−11 to +2, numbering relative to the start site base +1) in promoter DNA, placement of +1 template base in the active site of the enzyme, and subsequent conformational changes to form the stable open complex RP_o. Each of these steps provides a checkpoint for regulatory input.

Over the past decade, structural (X-ray, FRET), single-molecule, and rapid mixing kinetic studies have greatly advanced the understanding of this machinery and these steps. Key advances include: (*i*) elucidation of the RNAP architecture at atomic resolution (1–4); (*ii*) dissection of composite forward and backward rate constants for RP_o formation into individual rate and/or equilibrium constants for the steps leading to RP_o (5, 6); (*iii*) single-molecule measurements of DNA topological changes (7); (*iv*) real-time determination of hydroxyl radial (HO•) protection patterns of DNA during stable open complex (RP_o) formation (8–10); and (*v*) finding that unstable open complexes are stabilized by binding the initiating nucleoside triphosphate and greatly destabilized by the stress response factors ppGpp and DksA (11–13). These advances make it possible to address the key unresolved questions of initiation. How is the opening of 12–14 base pairs distributed between the steps of RP_o formation? Does RNAP disrupt the DNA duplex in the active site cleft or does DNA melt outside the channel and enter as individual strands?

Evidence for at least two kinetically significant intermediates (generically designated I_1 and I_2) preceding RP_o exists for a variety of promoters recognized by *E. coli* RNAP (cf. refs. 6, 8, and 14–17). Conversion of I_1 to I_2 is the rate-determining (bottleneck) step in forming the open complex at the λP_R promoter and exhibits a 34-kcal activation enthalpy barrier (17). The reverse direction of this step is the bottleneck step in dissociation of RP_o (6). Because I_1 is a closed complex (9), determining when DNA opens requires trapping I_2.

The minimal mechanism of RP_o formation is formally analogous to minimal mechanisms of solute transport through membranes and enzyme catalysis. All involve three steps in which the initial step in each direction is rapidly reversible and a middle step that is the bottleneck in both directions. In RP_o formation, as in mechanisms of catalysis and transport, ligands and solutes primarily act on the rapidly reversible steps and not on the central bottleneck step (6, 18). Given these analogies, is the central bottleneck step of open complex formation indeed DNA opening, just as transport is the central step in transporter mechanisms and catalysis is in enzyme mechanisms?

We address this fundamental mechanistic question by using a powerful method from physical enzymology, the burst experiment, which forms a transiently high concentration of an otherwise unobservable intermediate (preceding the bottleneck step). In the forward direction, a burst of I_1 is generated by rapid mixing with a sufficiently high [RNAP] (cf. Fig. 1*A*). HO• and permanganate (MnO_4^-) footprints of the population of the λP_R promoter DNA in such a forward burst experiment demonstrate that I_1 is a MnO_4^--unreactive complex in which downstream duplex DNA is protected to +20 from HO• attack (9). Structural modeling on the basis of these data and the X-ray structures of the bacterial RNAP (1, 2) indicates that duplex DNA in I_1 is loaded in the active site cleft of RNAP but not yet open (9).

Because the rate limiting forward step is the conversion of I_1 to I_2, no subsequent burst of I_2 occurs in the forward direction experiment (Fig. 1*A*). Hence the dissociation direction must be investigated to obtain a sufficient population of I_2 to characterize. The time course of a standard dissociation experiment in which a

Author contributions: T.J.G., W.S.K., R.M.S., and M.T.R. designed research; T.J.G., W.S.K., M.W.C., and R.M.S. performed research; T.J.G., R.M.S., and M.T.R. analyzed data; and T.J.G., R.M.S., and M.T.R. wrote the paper.

The authors declare no conflict of interest.

*This Direct Submission article had a prearranged editor.

[1]To whom correspondence may be addressed. E-mail: rmsaecker@wisc.edu or mtrecord@wisc.edu.

[2]Present address: Department of Bacteriology, Great Lakes Bioenergy Research Center, University of Wisconsin, 1550 Linden Drive, Madison, WI 53706.

This article contains supporting information online at www.pnas.org/lookup/suppl/doi:10.1073/pnas.1000967107/-/DCSupplemental.

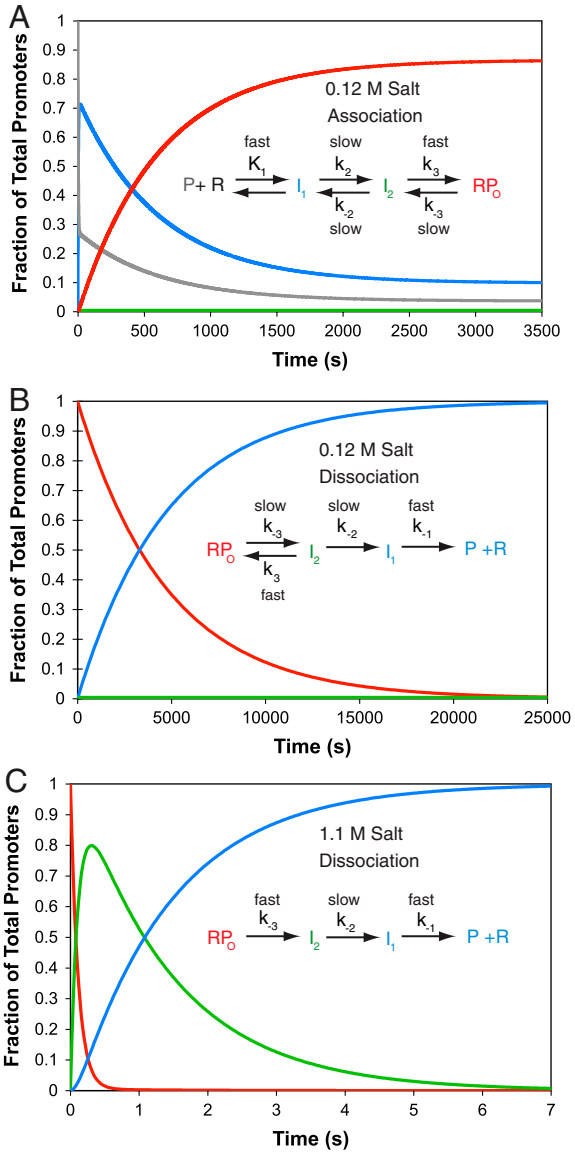

Fig. 1. A burst dissociation experiment is required to characterize the unstable intermediate I_2. Simulations of changes in the populations of RP_o (*Red*), I_2 (*Green*), I_1 (*Blue*), and free λP_R promoter DNA (P, *Gray*) at 10 °C, 0.01 M Mg^{2+} as a function of time are shown for: (*A*) reversible association at high [RNAP] (100 nM) and 0.12 M salt (KCl or NaCl); (*B*) irreversible (in excess competitor) dissociation at 0.12 M salt; and (*C*) irreversible dissociation after a rapid upshift to 1.1 M salt. Rate and equilibrium constants for the association simulation (*A*) are from ref. 17; at no point on the association time course is there a significant population of I_2. Rate and equilibrium constants for the dissociation simulations are from ref. 6. The salt upshift (*C*) produces a large transient burst of I_2, not observed in the low salt dissociation experiment (*B*). The species designated RP_o also includes a minor population of the late intermediate I_3 (6), which is not resolved from RP_o in the present studies. Values of the parameters used to generate these simulations are given in Table S1.

competitor such as heparin is added to make dissociation irreversible is shown in Fig. 1*B*. Because I_2 is an unstable intermediate, rapidly converting back to the stable open complex on the time scale of its conversion to I_1, it never accumulates to a significant level in this experiment. Kontur et al. (6) discovered that rapid destabilization of the stable open complex with moderately high concentrations of urea or salt generates a dramatic transient buildup (burst) of I_2 ~0.5 s after mixing (Fig. 1*C*). (A RP_o-destabilizing temperature downshift cannot be performed rapidly enough to detect such bursts.) Because the rate of conversion of I_2 to I_1 is found to be independent of urea or salt concentration, the burst of I_2 persists for a period of approximately 1 s, ample time for characterization of the extent of opening of bases in I_2 and of the decay of I_2 to I_1 by fast MnO_4^- footprinting.

In Fig. 1 (all panels) at 10 °C, the stable open complex (labeled RP_o) may be an equilibrium mixture containing some of the intermediate complex I_3 identified previously (6). An increase in the population of I_3 is expected early in the solute upshifts in Fig. 1*C*, decaying to I_2 in less than 100 ms. Simulations on the basis of kinetic data (6) show that the time resolution of the three-syringe burst/fast footprinting experiments reported in this research is insufficient to investigate I_3, and its population is therefore combined with that of RP_o in Fig. 1.

Results

To determine whether the DNA in I_2 is closed or partially or fully open in the region of the initiation bubble, we footprinted thymines with a constant dose of MnO_4^- (19). Complexes were probed as a function of time after rapidly destabilizing open complexes with 1.1 M NaCl or after mixing them with 0.12 M NaCl (control reaction). The sequencing gels in Fig. 2 compare the time-dependent behavior of all MnO_4^--reactive positions on each strand after the upshift with that of the control reaction.

For the template (t) strand (Fig. 2*A*) the control lanes indicate that thymines at positions +1, −8/ − 9 (doublet band), and −11 are MnO_4^--reactive in RP_o. After the upshift to 1.1 M NaCl, a monotonic decay of MnO_4^- reactivity of these bands is observed in the time range 0.1–10 s. For the nontemplate (nt) strand (Fig. 2*B*), the control lanes indicate that thymines at positions +2 and −3/ − 4 (doublet band) are MnO_4^--reactive in RP_o; the kinetics of the decay in MnO_4^- reactivity with time after

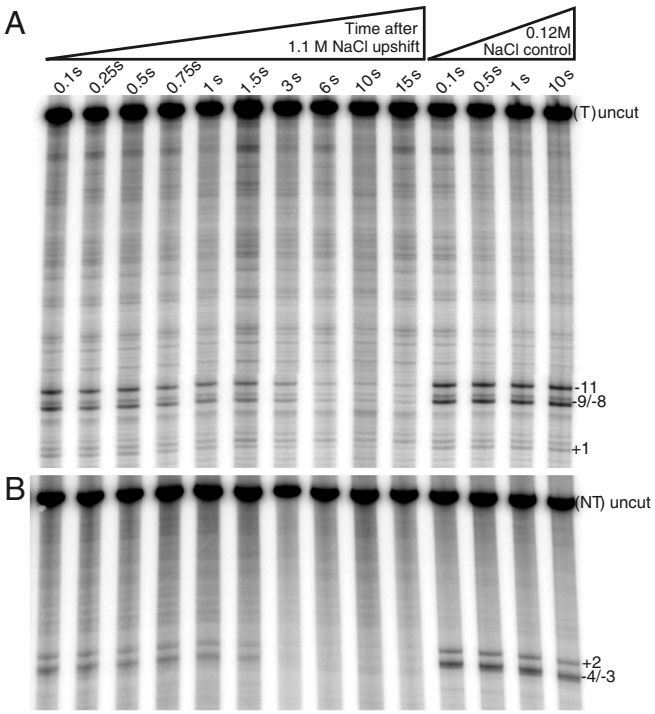

Fig. 2. Visualizing open thymines on template and nontemplate strands during the burst and subsequent decay of intermediate promoter complex I_2 after an upshift of RP_o to 1.1 M NaCl. Sequencing gels (representative of three independent experiments) show the decay of permanganate reactivity of individual open thymine bases (left lanes) on the template (*A*) and nontemplate (*B*) strands as a function of time after upshift, probed with a constant dose of $NaMnO_4$ (see *Material and Methods*). Right lanes show corresponding low salt RP_o reactivity controls for both strands as a function of time after mixing with 0.12 M NaCl.

the NaCl upshift is very similar to that of the t strand. Thymines at −7 and −10 on the nt strand are not detected, though the DNA is open in this region (as judged by reactivity at positions −11 and −8/ − 9 on the t strand). We infer that interactions of these upstream nt strand thymines with σ^{70} region 2 (cf. ref. 20 and references therein) protect them from reacting with MnO_4^- in I_2 as well as in RP_o.

In addition to providing visual demonstrations of the positions of reactive thymines in I_2 and of the time course of their decay as I_2 converts to products (I_1 and then free promoter DNA), Fig. 2 allows a visual comparison of the reactivities of these thymines in I_2 [judged by the early time points (0.1–0.25 s) after the upshift], both relative to other thymines in I_2 and to the RP_o control. At 0.25 s, the population distribution of promoter DNA (Fig. 3*A*) is 80% I_2, 10% RP_o and I_3, and 10% closed I_1 and free promoter DNA. Strikingly, in the early time lanes where I_2 is the major species, thymines at both +2 and −3/ − 4 on the nt strand appear much less reactive than in the RP_o control, whereas reactive thymines at +1 and other positions on the t strand appear nearly as reactive as in the RP_o control.

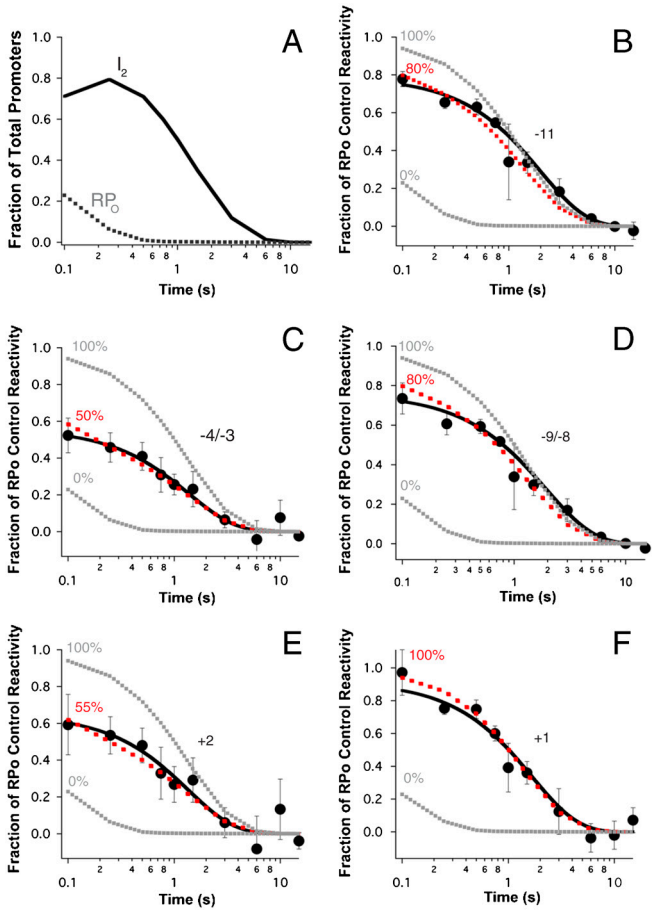

Fig. 3. Kinetics of the open to closed transition of individual thymines as the burst population of I_2 decays to I_1 and promoter DNA. (*A*) Predicted populations of RP_o and I_2 (see *SI Text*) are plotted versus time (log scale) after NaCl upshift (0.1–10 s). (*B–F*) Relative MnO_4^- reactivities of each thymine singlet or doublet band (calculated from three independent experiments on each strand; see Fig. 2) as a function of time (log scale). Solid curves are single exponential fits of these data, yielding the rate constants for the decay of I_2 in Table 1. Simulations of the decay using the population distribution in Fig. 1*C* and varying the MnO_4^- reactivity of each thymine singlet or doublet in I_2 relative to the RP_o control are shown as dashed lines. The best fit is shown in red; the limits of the fit (I_2 closed (0% reactive) and I_2 as open as RP_o (100%)) are shown in gray.

To explore the behavior of each MnO_4^--reactive thymine during dissociation, we quantified their individual decay kinetics and reactivities relative to the RP_o control (Fig. 3 and Table 1). In Fig. 3*A*, the populations of I_2 and of RP_o (including I_3) are plotted as a function of time after the upshift on a logarithmic time scale (two decades, from 0.1 to 10 s) to compare with the analysis of the individual thymines shown in the subsequent panels. For all thymines, the observed change in MnO_4^- reactivity is well fit by a single exponential decay (*Solid Curve*, Fig. 3 *B–F*). Although I_2 is initially the dominant species after the upshift, the presence of some RP_o, I_3, and closed promoter DNA requires that the data be deconvoluted to quantify the MnO_4^- reactivity of each thymine in I_2. A series of simulations of the observed decay kinetics were performed in which these reactivities were systematically varied from 0% (unreactive in I_2) to 100% (as reactive in I_2 as in RP_o). Simulated time courses calculated by using the best-fit reactivities of each thymine in the bubble in I_2 are compared with the 0% and 100% limiting cases and with the experimental data in Fig. 3 *B–F*. Best-fit reactivities are listed in Table 1 together with the rate constants for decay of each reactive thymine in the conversion of I_2 to I_1.

Comparison of the results reveals that:

i. Decay rate constants are the same for all thymines ($0.6 \pm 0.1\ s^{-1}$) and agree within the uncertainty with the rate constant for the conversion of I_2 to I_1 ($k_{-2} = 0.72 \pm 0.07\ s^{-1}$) determined by filter binding of quenched samples as a function of time after exposure to a 1.1 M salt upshift (6).

ii. The MnO_4^- reactivity of the start site (+1) thymine on the t strand in I_2 is the same as in the RP_o control. MnO_4^- reactivities of upstream thymines on the t strand in I_2 are about 80% as large as in the RP_o control. MnO_4^- reactivities of downstream thymines on the nt strand in I_2 are 50–55% as large as in the RP_o control. (These conclusions are insensitive to assumptions regarding the amount and MnO_4^- reactivity of the I_3 present in the residual population labeled RP_o in Fig. 3*A*) Thymines at −7 and −10 on the nt strand are fully protected (zero MnO_4^- reactivity) in both I_2 and RP_o.

Discussion

Opening of the Initiation Bubble Occurs in the Active Site Cleft to Convert the Closed Complex I_1 to I_2. The architecture of multisubunit RNA polymerases appears to have evolved a series of steric blocks to prevent access of nonpromoter DNA to the active site (2–4, 9, 21, 22). For example, bacterial RNAP recognizes promoter DNA by interactions between the σ subunit and hexameric sequences (−10 and −35 regions) that are upstream of +1 (cf. ref. 23 and references therein). Placement of σ^{70} with respect to the channel requires the DNA to bend sharply at −11/ − 12 to enter the active site cleft formed by the β and β′ "pincers" (or jaws) (2, 17). Does double-stranded DNA bind in the cleft at this point in the mechanism prior to being opened by RNAP? Or does the DNA open above the cleft, allowing the template strand to then descend down to the active site "floor" (2, 23)?

The relatively "closed" state of the pincers (less than 25 Å apart) observed in crystal structures of the bacterial RNAP (2, 22) and the transcription factor TFIIB bound to the 12-subunit eukaryotic RNAP (24, 25) has motivated proposals that DNA must open outside of the cleft. For the bacterial RNAP, which lacks a helicase cofactor, opening outside the active site cleft is proposed to be nucleated by a thermal breathing mechanism (23). In this proposal, transient opening and closing of the A/T-rich −10 hexamer leads to capture of the nt strand by σ^{70} region 2 at the upstream entrance (23), followed by entry of only the t strand into the cleft (2, 23). Indeed an RNAP subassembly consisting of σ^{70} region 2 and an N-terminal fragment of β′ was observed to form an open (MnO_4^--reactive) complex with a highly A/T-rich promoter set in negatively supercoiled DNA; this

Table 1. Permanganate reactivities of thymine bases in the open region of I_2 and rate constants for closing these positions in I_2 to I_1

Strand	Template			Nontemplate	
Position	−11	−9/−8	+1	−4/−3	+2
Rate constant (s^{-1})*	0.50 (±0.04)	0.52 (±0.05)	0.6 (±0.1)	0.7 (±0.2)	0.7 (±0.3)
Predicted reactivity of I_2 (relative to RP_o control)†	80%	80%	100%	50%	55%

*Fit parameters from the decay kinetics (solid lines) in Fig. 3. The rate constant for the conversion of I_2 to I_1 (k_{-2}) determined by nitrocellulose filter-binding experiments at 10 °C is 0.72 (±0.07) s^{-1} (6).

†Uncertainty in these reactivities, estimated from the range of triplicate determinations at a given time point in the range from 0.1 to 0.75 s, is ±10%. See *Material and Methods*.

polymerase subassembly did not open this promoter on linear DNA (26). Whereas these structure- or equilibrium-based mechanistic hypotheses are appealing and could apply to promoters under highly negative supercoiling stress and/or high temperature, *E. coli* RNAP readily forms open complexes on linear promoter fragments in vitro.

Kinetic-mechanistic studies of RP_o formation and dissociation at the λP_R promoter combined with footprinting data argue that interactions of regions of *E. coli* RNAP with promoter DNA bound in the cleft actively distort and open the initiation bubble. HO• and DNase I cleavage of the DNA backbone of the early intermediate I_1 demonstrate that both the t and nt DNA strands are protected without interruption in this region (−15 to +25), whereas MnO_4^- does not detect any unstacked thymine bases (9, 27, 28). For the T7A1 promoter, time-resolved HO• footprints of populations of intermediates during formation of stable open complexes have been interpreted in terms of a mechanism involving three classes of intermediates before the rate-determining step (10). Comparison of the kinetics of development of downstream MnO_4^- reactivity with the kinetics of downstream HO• protection led the authors to propose that DNA opening occurs outside the cleft and before the rate-determining step (10). Further research is needed to determine the nature of the rate-determining step at T7A1 and to understand the origins of the apparent mechanistic differences between these two promoters.

Experiments presented here demonstrate that MnO_4^--reactive thymines appear in the conversion of I_1 to I_2 at λP_R. We conclude from these results that the pincers of RNAP are sufficiently flexible in solution to allow DNA to enter as a double helix, where it is then opened via binding interactions with elements on RNAP. Additional evidence that DNA opening occurs in the active site cleft and not in solution is provided by the observation that the [salt] dependence of the DNA opening step (conversion of I_1 to I_2) is much smaller in magnitude than that of melting 12–14 base pairs of DNA in solution (18). We proposed that the N-terminal polyanionic domain of σ^{70} (σ region 1.1) must move in the cleft, allowing the duplex DNA to descend (18). These movements would position $-2/-1$(t) near the highly conserved region on the downstream lobe of β known as fork loop 2. By analogy with base-flipping enzymes, we speculate that fork loop 2 inserts in the minor groove, creating a 90° bend and unwinding the DNA helix to form the I_1-I_2 transition state. Interactions between the DNA phosphate backbone and positive regions in the cleft provide an additional driving force for opening. A *bind-bend-open* mechanism has also been proposed for RP_o formation by the single subunit T7 phage RNAP and tested by stopped flow kinetic and FRET experiments (29, 30).

Single-molecule DNA magnetic tweezer experiments revealed that unwinding of ~1 turn of the helix in an *E. coli* RNAP–promoter complex occurred in a single process at all promoters studied on both negatively and positively supercoiled DNA (7). Because the time resolution of the assay was ~1 s, these experiments could not resolve whether untwisting occurred in a single kinetic step, or whether the mechanism involved a sequence of unwinding steps. Our results show that opening (unpairing, partial unstacking, and therefore unwinding) occurs in the bottleneck step of RP_o formation (I_1 to I_2) at the λP_R promoter.

Proposed DNA Conformations in the Steps in Open Complex Formation. Fig. 4 shows a schematic of the proposed series of conformational changes in the downstream DNA in the RNAP active site channel as the reaction proceeds from the closed intermediate I_1 to the unstable open complex I_2 and finally to the stable open complex RP_o. DNA in I_1 is shown as double-stranded with the exception of a distortion at −11(t), which flips out −11A(nt) (20). However, because −11(t) is not MnO_4^--reactive, we infer that it remains stacked with other DNA bases and/or is interacting with RNAP (9). In our model of I_1, the +1 base pair lies ~40 Å above the active site Mg^{2+} (9, 17). Further descent of duplex DNA in I_1 is blocked by σ region 1.1 and the β′ "bridge" helix that spans the channel.

Because the MnO_4^- reactivity of +1 appears to be the same in both I_2 and RP_o, we propose that opening of the bubble in $I_1 \rightarrow I_2$ places the +1(t) base in the active site (near the catalytic Mg^{2+}). However, the reduced reactivities of other thymines, especially those on the nt strand (Table 1), motivate the proposal that the surrounding protein environment and/or degree of stacking of these thymines in I_2 differs from that in RP_o. Large conformational changes in RNAP accompany the conversion of I_2 to RP_o (5, 15). Very large solute effects on the dissociation rate constant k_d and the large activation heat capacity of k_d provide evidence that the downstream clamp/jaw is assembled and tightened on the downstream DNA duplex (+5 to +20) in these late steps of RP_o formation, *after* the DNA has been opened (6, 18, 31) (see Fig. 4). The twofold increase in permanganate reactivity of nt strand thymines at $-4/-3$ and +2 in the conversion of I_2 to RP_o indicates that the nt strand is repositioned and/or unstacked in these steps. These local changes in the nt strand in the cleft may be coupled to changes in positioning of σ^{70} region 1.1 and the switch regions (3, 32) and to the large scale downstream conformational changes involved in assembly and DNA binding

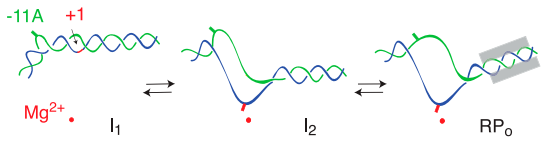

Fig. 4. Proposal for DNA conformational changes during the steps of opening and stabilizing the initiation bubble at the λP_R promoter. Proposed location (relative to the active site Mg^{2+}, shown as a red dot) and extent of bending and/or opening of DNA strands (template, blue; nontemplate, green; −20 to +20) in the bent and wrapped closed complex I_1, in the relatively unstable initial open complex I_2, and in the stable open complex RP_o. The transcription start site thymine is shown as a red rectangle. −11A (*Green Rectangle*) on the nontemplate strand is proposed to be flipped out in the 90° bend that directs the duplex into the active site cleft in I_1. Formation of I_1 loads downstream duplex in the active site cleft. RNAP opens the DNA in the cleft and positions the t strand start site base (+1) in the active site, forming I_2. Final loading of the nt strand and assembly of a clamp/jaw (*Gray Rectangles*) on the downstream duplex DNA greatly stabilize RP_o relative to I_2.

of the clamp/jaw. Together these events greatly stabilize RP_o relative to I_2.

Opening of the entire bubble (−11 to +2) is rate-determining at the λP_R promoter and has the properties of a single (elementary) kinetic step. At other promoters, opening may be separated into several kinetically distinguishable steps and may or may not be rate-determining (10, 20). For the λP_R promoter, the activation enthalpy barrier is very high for the forward direction of the opening step [34 kcal; (17)]; and the overall enthalpy change for this step is also large [~24 kcal; (6)]. For comparison, the enthalpy of melting 13 bp of DNA in solution is approximately 75 kcal at 25 °C (33). One interpretation of the 34-kcal activation barrier is that approximately half the bubble is open and unstacked in the transition state and that few enthalpically favorable interactions with RNAP have formed at this stage. Alternatively, the majority of bases in the bubble may be unpaired but not unstacked or, if unstacked, may be engaged in enthalpically favorable interactions with RNAP. Opening in the cleft is likely initiated at the −11 bend by interactions between the −10 region of the nt strand and aromatic residues of σ^{70} region 2 (20). Because these interactions presumably are enthalpically favorable, we infer that the majority of the bubble is open in the transition state. Conversion of this very unstable transition state to I_2 likely establishes additional interactions with RNAP, possibly including those between the t strand and switch 2 of β′ (32).

Proposed Physiological Relevance of the Unstable Open Complex I_2. Under physiological conditions, I_2 is highly unstable relative to RP_o at the λP_R promoter and converts to RP_o so rapidly that it never accumulates (Fig. 1 *A* and *B*). Yet the conversion of I_1 to I_2 opens the entire transcription bubble and may correctly load the start site base in the active site. Do multiple open complexes (RP_o, I_3, and I_2) with large differences in stability play distinct functional roles in the regulation of transcription initiation? We propose that the answer to this question is strongly affirmative.

Extensive studies of transcription initiation at the ribosomal *rrnB* P1 promoter by Gourse, Ross, and coworkers reveal that the open complex formed at this promoter in the absence of NTPs and negative supercoiling is highly unstable, with a short lifetime, existing in an equilibrium shifted toward closed complexes (cf. ref. 34 and references therein). If open complex formation at λP_R were blocked at I_2 or I_3, unable to progress to the stable RP_o, then a similar situation would be observed. An equilibrium would exist between these unstable open intermediates and the closed complex I_1 shifted toward I_1 at 25 °C and with a lifetime of I_2 of only a few seconds. On the basis of this kinetic/thermodynamic analogy, and because I_2 at λP_R and the functional open complex at *rrnB* P1 both appear to be the first open complex formed from a closed complex at these promoters, we propose that the unstable intermediate(s) I_2 (and/or I_3) at λP_R behave functionally and structurally like the unstable open complex characterized at *rrnB* P1.

A key functional property of the open complex at *rrnB* P1 is the ability to initiate synthesis of a full-length transcript rapidly and efficiently, without any short, abortive product synthesis, upon addition of all four NTPs (35). A key structural property of the *rrnB* P1 open complex is its shorter downstream boundary of the hydroxyl radical footprint (~ + 12 to +15 of the (t) strand for the *rrnB* P1 (36), compared to +20 to +25 for RP_o at λP_R (9). This difference in downstream boundaries likely reflects a difference in the extent of assembly and DNA binding of downstream mobile domains in β′ including the clamp, jaw, and sequence insertion 3, which we propose stabilize RP_o at λP_R (6, 18, 31). We hypothesize that these hallmarks of the open complex at *rrnB* P1 will be observed for I_2 (and/or I_3) at λP_R.

The instability (relative to the closed complex) and short lifetime of the open complex at ribosomal promoters makes it a target of regulation by proteins like DksA (12) and by ligands including the stress factor ppGpp (37, 38) and the initiating NTP (11). Clearly, ribosomal expression has been tuned to respond rapidly to changes in conditions, including changes in NTP concentrations. We hypothesize that complete assembly and tightening of the clamp/jaw on downstream DNA characteristic of the stable open complex RP_o at λP_R is disfavored at the *rrnB* P1 promoter [possibly because of differences in interactions with the nt strand in the cleft (39, 40)], explaining its instability relative to λP_R. If so, tight downstream interactions would not need to be broken for RNAP to escape from the *rrnB* P1 promoter, allowing highly efficient production of full-length transcripts under exponential growth conditions. In contrast, a fully assembled and tightened clamp at λP_R in RP_o may impede escape and favor abortive initiation, consistent with the observation that downstream DNA from +1 to +20 plays a key role in determining the efficiency of the transition to elongation (41).

For a series of promoters that form stable binary open complexes, Hsu, Chamberlin and colleagues obtained evidence for two ternary initial transcription complexes (ITCs): One ITC makes only abortive products and the other primarily makes full length transcripts. For these promoters, the overall abortive:productive ratio is large and promoter-sequence-dependent [(42); see also ref. 43]. Abortive transcripts are made in vivo (44); their cellular function as small RNAs is not yet known.

What is the relationship between multiple binary open complexes (I_2, I_3, and RP_o) and multiple ITCs? We propose that stable RP_o, with its tightly gripping downstream clamp/jaw, is capable of only abortive synthesis, whereas less-stable I_2 and I_3, in which the clamp/jaw is less assembled and/or less tightly bound to downstream DNA, are capable of productive initiation. In this model, the relative populations of stable (RP_o) and less stable (I_2 and I_3) open complexes determine the observed abortive:productive ratio. The fact that the clamp/jaw assembles only after DNA opening and untwisting is complete indicates that its grip likely impedes the movement of duplex DNA within it. Promoter sequence, sigma factor, concentrations of regulatory ligands, and solution conditions all must affect the relative stability and lifetime of each initiation intermediate and hence are determinants of initiation rate and the abortive:productive ratio, providing potent and relatively unexplored avenues for the regulation of transcription.

Material and Methods

Solutions and Materials. Standard methods of purifying RNAP and of obtaining ^{32}P-labeled DNA fragments were used. See *SI Text*.

High [NaCl] Fast-Kinetic MnO_4 DNA Footprinting. Labeled DNA promoter fragments in BB were mixed with RNAP in SB at a final concentration of 10 nM and incubated at room temperature (~20 °C) for 90 min to preform open complexes. These complexes were loaded into the *sample A* tube of a KinTek Corporation RQF-3 Rapid Chemical Quench-Flow instrument cooled to 10 °C by a circulating water bath. *Push syringe A* was loaded with BB supplemented to 4% SB. The *sample B* tube and *push syringe B* were loaded with BB supplemented to 1.96 M NaCl, 400 μg/mL heparin, and 4% SB. *Push syringe C* was loaded with a solution containing 200 mM $NaMnO_4$ and 900 mM NaCl. Collection tubes were filled with 300 μL of a quench solution containing 3.75 M ammonium acetate and 7.1 M β-mercaptoethanol. The quench-flow instrument was operated in a *push-pause-push-pause-push* mode. The first push rapidly mixed the preformed open complexes with the high salt solution resulting in a final [NaCl] of 1.1 M. This solution was held in *reaction loop 7* for the desired perturbation time. The second push mixed the contents of reaction loop with the solution in *push syringe C* resulting in a final [MnO_4^-] of 66.7 mM. This solution was held in the *exit tube* for 150 ms before the final push expelled the solution into the collection tube containing quench solution. Quenched reac-

tions were immediately ethanol precipitated. Each load–reaction cycle took 250 min. Low salt control reactions were performed as above with the exception of loading solutions that keep [NaCl] at 120 mM. DNA fragments were washed with 70% ethanol, resuspended, reprecipitated, and washed. Modified fragments were cleaved by incubation at 90 °C in 1 M piperidine. Reactions were evaporated and resuspended in TE buffer (10 mM Tris HCl, 1 mM EDTA, pH 8.0) three times. The resulting DNA was resuspended in urea loading buffer and resolved on an 8% acrylamide gel. The gel was dried and exposed to a storage phosphor screen. The screen was scanned on a Typhoon scanner, and the resulting data analyzed with ImageQuant software. Phosphoimager intensities of each MnO_4^- reactive thymine band (or doublet) as a function of time after the salt upshift were fit to a first order (single exponential) rate equation in which the long-time plateau value was floated. To obtain normalized θ values [fraction of that base remaining in an open (I_2) condition], this long-time plateau intensity, arising from background/duplex reactivity of the thymine, was subtracted from the observed phosphoimager intensity at each time and divided by the background corrected intensity of that position in a low salt RP_o control. Data fitting was performed by using IgorPro 5 software.

Population Modeling. See *SI Text*.

ACKNOWLEDGMENTS. We thank Dr. C. Davis for preliminary $KMnO_4$ experiments. We are grateful to our colleagues for many fruitful discussions and to the reviewers and the editor for their comments on the manuscript. This work was supported by National Institutes of Health Grant GM23467 (to M.T.R.). T.J.G. gratefully acknowledges the support of the William R. and Dorothy E. Sullivan Distinguished Graduate Fellowship. W.S.K. acknowledges support from National Institutes of Health Biotechnology Training Grant (NIH 5 T32 GM08349).

1. Murakami KS, Masuda S, Darst SA (2002) Structural basis of transcription initiation: RNA polymerase holoenzyme at 4 Å resolution. *Science* 296:1280–1284.
2. Vassylyev DG, et al. (2002) Crystal structure of a bacterial RNA polymerase holoenzyme at 2.6 Å resolution. *Nature* 417:712–719.
3. Cramer P, Bushnell DA, Kornberg RD (2001) Structural basis of transcription: RNA polymerase II at 2.8 Å resolution. *Science* 292:1863–1876.
4. Zhang G, et al. (1999) Crystal structure of *Thermus aquaticus* core RNA polymerase at 3.3 Å resolution. *Cell* 98:811–824.
5. Saecker RM, Record MT, Jr (2002) Protein surface salt bridges and paths for DNA wrapping. *Curr Opin Struct Biol* 12:311–319.
6. Kontur WS, Saecker RM, Capp MW, Record MT, Jr (2008) Late steps in the formation of *E. coli* RNA polymerase—λP_R promoter open complexes: characterization of conformational changes by rapid [perturbant] upshift experiments. *J Mol Biol* 376:1034–1047.
7. Revyakin A, Ebright RH, Strick TR (2004) Promoter unwinding and promoter clearance by RNA polymerase: detection by single-molecule DNA nanomanipulation. *Proc Natl Acad Sci USA* 101:4776–4780.
8. Sclavi B, et al. (2005) Real-time characterization of intermediates in the pathway to open complex formation by *Escherichia coli* RNA polymerase at the T7A1 promoter. *Proc Natl Acad Sci USA* 102:4706–4711.
9. Davis CA, Bingman CA, Landick R, Record MT, Jr, Saecker RM (2007) Real-time footprinting of DNA in the first kinetically significant intermediate in open complex formation by *Escherichia coli* RNA polymerase. *Proc Natl Acad Sci USA* 104:7833–7838.
10. Rogozina A, Zaychikov E, Buckle M, Heumann H, Sclavi B (2009) DNA melting by RNA polymerase at the T7A1 promoter precedes the rate-limiting step at 37 °C and results in the accumulation of an off-pathway intermediate. *Nucleic Acids Res* 37:5390–5404.
11. Gaal T, Bartlett MS, Ross W, Turnbough CL, Jr, Gourse RL (1997) Transcription regulation by initiating NTP concentration: rRNA synthesis in bacteria. *Science* 278:2092–2097.
12. Paul BJ, et al. (2004) DksA: a critical component of the transcription initiation machinery that potentiates the regulation of rRNA promoters by ppGpp and the initiating NTP. *Cell* 118:311–322.
13. Paul BJ, Berkmen MB, Gourse RL (2005) DksA potentiates direct activation of amino acid promoters by ppGpp. *Proc Natl Acad Sci USA* 102:7823–7828.
14. Buc H, McClure WR (1985) Kinetics of open complex formation between *Escherichia coli* RNA polymerase and the lacUV5 promoter. Evidence for a sequential mechanism involving three steps. *Biochemistry* 24:2712–2723.
15. Roe JH, Burgess RR, Record MT, Jr (1985) Temperature dependence of the rate constants of the *Escherichia coli* RNA polymerase—λP_R promoter interaction. Assignment of the kinetic steps corresponding to protein conformational change and DNA opening. *J Mol Biol* 184:441–453.
16. Li XY, McClure WR (1998) Characterization of the closed complex intermediate formed during transcription initiation by *Escherichia coli* RNA polymerase. *J Biol Chem* 273:23549–23557.
17. Saecker RM, et al. (2002) Kinetic studies and structural models of the association of *E. coli* σ^{70} RNA polymerase with the λP_R promoter: Large scale conformational changes in forming the kinetically significant intermediates. *J Mol Biol* 319:649–671.
18. Kontur WS, Capp MW, Gries TJ, Saecker RM, Record MT, Jr (2010) Probing DNA binding, DNA opening and assembly of a downstream clamp/jaw in *Escherichia coli* RNA polymerase—λP_R promoter complexes using salt and the physiological anion glutamate. *Biochemistry*, in press.
19. Borowiec JA, Zhang L, Sasse-Dwight S, Gralla JD (1987) DNA supercoiling promotes formation of a bent repression loop in lac DNA. *J Mol Biol* 196:101–111.
20. Schroeder LA, et al. (2009) Evidence for a tyrosine-adenine stacking interaction and for a short-lived open intermediate subsequent to initial binding of *Escherichia coli* RNA polymerase to promoter DNA. *J Mol Biol* 385:339–349.
21. Bushnell DA, Kornberg RD (2003) Complete, 12-subunit RNA polymerase II at 4.1 Å resolution: Implications for the initiation of transcription. *Proc Natl Acad Sci USA* 100:6969–6973.
22. Murakami KS, Masuda S, Campbell EA, Muzzin O, Darst SA (2002) Structural basis of transcription initiation: An RNA polymerase holoenzyme-DNA complex. *Science* 296:1285–1290.
23. Murakami KS, Darst SA (2003) Bacterial RNA polymerases: The wholo story. *Curr Opin Struct Biol* 13:31–39.
24. Kostrewa D, et al. (2009) RNA polymerase II-TFIIB structure and mechanism of transcription initiation. *Nature* 462:323–330.
25. Liu X, Bushnell DA, Wang D, Calero G, Kornberg RD (2010) Structure of an RNA polymerase II-TFIIB complex and the transcription initiation mechanism. *Science* 327:206–209.
26. Young BA, Gruber TM, Gross CA (2004) Minimal machinery of RNA polymerase holoenzyme sufficient for promoter melting. *Science* 303:1382–1384.
27. Craig ML, et al. (1998) DNA footprints of the two kinetically significant intermediates in formation of an RNA polymerase-promoter open complex: evidence that interactions with start site and downstream DNA induce sequential conformational changes in polymerase and DNA. *J Mol Biol* 283:741–756.
28. Davis CA, Capp MW, Record MT, Jr, Saecker RM (2005) The effects of upstream DNA on open complex formation by *Escherichia coli* RNA polymerase. *Proc Natl Acad Sci USA* 102:285–290.
29. Tang GQ, Patel SS (2006) Rapid binding of T7 RNA polymerase is followed by simultaneous bending and opening of the promoter DNA. *Biochemistry* 45:4947–4956.
30. Tang GQ, Patel SS (2006) T7 RNA polymerase-induced bending of promoter DNA is coupled to DNA opening. *Biochemistry* 45:4936–4946.
31. Kontur WS, Saecker RM, Davis CA, Capp MW, Record MT, Jr (2006) Solute probes of conformational changes in open complex (RP_o) formation by *Escherichia coli* RNA polymerase at the λP_R promoter: Evidence for unmasking of the active site in the isomerization step and for large-scale coupled folding in the subsequent conversion to RP_o. *Biochemistry* 45:2161–2177.
32. Belogurov GA, et al. (2009) Transcription inactivation through local refolding of the RNA polymerase structure. *Nature* 457:332–335.
33. Holbrook JA, Capp MW, Saecker RM, Record MT, Jr (1999) Enthalpy and heat capacity changes for formation of an oligomeric DNA duplex: interpretation in terms of coupled processes of formation and association of single-stranded helices. *Biochemistry* 38:8409–8422.
34. Haugen SP, Ross W, Gourse RL (2008) Advances in bacterial promoter recognition and its control by factors that do not bind DNA. *Nat Rev Microbiol* 6:507–519.
35. Gourse RL (1988) Visualization and quantitative analysis of complex formation between *E. coli* RNA polymerase and an rRNA promoter in vitro. *Nucleic Acids Res* 16:9789–9809.
36. Rutherford ST, Villers CL, Lee JH, Ross W, Gourse RL (2009) Allosteric control of *Escherichia coli* rRNA promoter complexes by DksA. *Genes Dev* 23:236–248.
37. Barker MM, Gaal T, Gourse RL (2001) Mechanism of regulation of transcription initiation by ppGpp. II. Models for positive control based on properties of RNAP mutants and competition for RNAP. *J Mol Biol* 305:689–702.
38. Barker MM, Gaal T, Josaitis CA, Gourse RL (2001) Mechanism of regulation of transcription initiation by ppGpp. I. Effects of ppGpp on transcription initiation in vivo and in vitro. *J Mol Biol* 305:673–688.
39. Haugen SP, et al. (2006) rRNA promoter regulation by nonoptimal binding of sigma region 1.2: An additional recognition element for RNA polymerase. *Cell* 125:1069–1082.
40. Feklistov A, et al. (2006) A basal promoter element recognized by free RNA polymerase sigma subunit determines promoter recognition by RNA polymerase holoenzyme. *Mol Cell* 23:97–107.
41. Hsu LM, Vo NV, Kane CM, Chamberlin MJ (2003) In vitro studies of transcript initiation by *Escherichia coli* RNA polymerase. 1. RNA chain initiation, abortive initiation, and promoter escape at three bacteriophage promoters. *Biochemistry* 42:3777–3786.
42. Vo NV, Hsu LM, Kane CM, Chamberlin MJ (2003) In vitro studies of transcript initiation by *Escherichia coli* RNA polymerase. 2. Formation and characterization of two distinct classes of initial transcribing complexes. *Biochemistry* 42:3787–3797.
43. Kubori T, Shimamoto N (1996) A branched pathway in the early stage of transcription by *Escherichia coli* RNA polymerase. *J Mol Biol* 256:449–457.
44. Goldman SR, Ebright RH, Nickels BE (2009) Direct detection of abortive RNA transcripts in vivo. *Science* 324:927–928.